Proceedings of GT2006
ASME Turbo Expo 2006: Power for Land, Sea and Air
May 8-11, 2006, Barcelona, Spain

GT2006-90011

Comparative Investigation of Advanced Combined Cycles

Hiwa Khaledi
Research Assistant
Sharif Energy Research Institute (SERI)
Sharif University of Technology
Tehran, 11365-9567, Iran
Email: khaledi@mehr.sharif.edu

Kazem Sarabchi
Associate Professor
Department of Mechanical Engineering
University of Tabriz
Tabriz, 11365-9567, Iran
Email: Sarabchi@tabrizu.ac.ir

ABSTRACT

Combined cycles, at present, have a prominent role in the power generation and advanced combined cycles efficiencies have now reached to 60 percent. Examination of thermodynamic behavior of these cycles is still carried out to determine optimum configuration and optimum design conditions for any cycle arrangement. Actually the performance parameters of these cycles are under the influence of various parameters and therefore the recognition of the optimum conditions is quiet complicated.

In this research an extensive thermodynamic model was developed for analyzing major parameters variations on gas turbine performance and different configurations of advanced steam cycles: dual and triple pressure cycles with and without reheating in steam turbine sections. In this model it is attempted to consider all factors that affect on actual behavior of these cycles such as blade cooling (air cooling) in gas turbine and different formulations for Heat Recovery Steam Generator (HRSG) performance calculation. Results show good agreement with manufactures data. In the case of gas turbine cycle, location of coolant extraction has large influence on cycle performance. For extraction from compressor end, improving blade cooling technology is suitable than increasing TIT. For mid stage extraction, improving blade cooling technology and TIT has similar effects on efficiency, while power is more sensitive to TIT. Coolant air precooling has large positive effect in high TIT and medium blade cooling technology, but always it increases power. Turbine exhaust temperature has large influence on optimum layout and configuration of HRSG, while for low exhaust temperatures increasing number of pressure levels increase power and heat recovery greatly, for high exhaust temperatures this leads lower enhancement in power and recovery. Second law efficiency of HRSG is proportional to power production in steam cycle. It decreases with increasing gas turbine exhaust temperature.

NOMENCLATURE

A, Ag, Aw	Area, gas path, wall path
C_p	Specific heat at constant pressure (kJ/kg.K)
DP	Pressure Drop
f	Fuel air ratio (mass basis)
h	Specific Enthalpy (kJ/kg)
ISO	ISO condition (15°C, 1.015 bar, 60% relative humidity)
LHV	Lower Heating Value (kJ/kg)
m	mass flow rate (kg/s)
m_H	Ratio of HP to total mass flow in HRSG
m_L	Ratio of LP to total mass flow in HRSG
MW	Molecular weight
M_a	Mach number
P	Pressure (bar)
q_{st}	total energy delivered to steam in HRSG per total steam mass flow (kJ/kg)
R	Gas constant (kJ/kmol.K)
s	Specific Entropy (kJ/kg.K)
St	Stanton Number
T	Temperature (°C)
ΔT	Temperature Difference

Subscripts

A	air
AP	Approach Point
$Amb.$	Ambient
Act	actual
B	blade
C	coolant
$cond.$	condenser
$C.C.$	Combustion Chamber
$C.P.$	Combustion Products
Exh	exhaust
f	saturation liquid
g	saturation vapor
$gen.$	generator
$g.b.$	Gear box
G	Gas
PP	Pinch Point
M	Mixture
$mech.$	mechanical
RH	ReHeater
sat	saturation

sup	superheat
st.	stack
wec	exit of economizer

Abbreviations

BD	Blow Down
CAP	Coolant Air Precooling
CC	Combined Cycle
CMF	Coolant Mass Flow
CEE	Compressor Exhaust Extraction
CME	Compressor Mid Extraction
ECO	Economizer
FPH	Fuel PreHeating
GT	Gas Turbine
HP	High pressure
HRSG	Heat Recovery Steam Generator
IP	Intermediate Pressure
LP	Low pressure
SC	Steam Cycle
SUP	Superheater
TIT	Turbine Inlet Temperature
TET	Turbine Exhaust Temperature

Greek symbols

$\bar{\lambda}$	Fuel to air mole fraction
η_{∞}	Polytropic Efficiency (c: compressor, t: turbine)
η_{is}	Isentropic Efficiency
η_{cc}	Combustion Chamber efficiency
ε	Heat exchanger efficiency (blade)
σ	Non dimensional parameter (blade cooling)

INTRODUCTION

Gas turbine based cycles are continually increasing their share in power and utility market. Different layouts for gas turbine cycles are analyzed including intercooling and aftercooling in compressor, recuperation, steam injection in combustion chamber and reheat in gas turbine [1], [2] and [3]. Novel cycles like humid air turbine (HAT) cycles can reach high efficiency and power due to good recovery of heat in low temperatures [4], [5]. But combined cycle power plants yet are the best option to produce power with high efficiency. Current combined cycles using closed loop steam blade cooling in gas turbine reached 60% efficiency [6] while it can increase to 61.2% [7].

Combined cycle efficiency usually increase in two ways together; first increasing turbine inlet temperature (TIT) (enhancement in blade cooling technology or maximum material temperature) and second by maximizing heat recovery in HRSG [8]. Increasing TIT is an expensive high tech work while maximizing heat recovery is simpler. Many researchers have focused on improvement of blade cooling technology and increasing TIT to enhance gas turbine performance [6], [9], but these enhancements change gas turbine exhaust conditions and modifications in design of HRSG must be considered.

Many researchers believe that with current technology, without increasing TIT and enhancement of blade cooling technology (i.e., closed loop steam blade cooling), achieving 60% efficiency is possible with optimization in HRSG [10], [11]. They have optimized HRSG for one special gas turbine without creating general rules for HRSG optimization.

In this study, gas turbine has been modeled considering cooling of turbine blades. Using this model effect of variations in TIT, blade cooling technology, location of coolant air extraction, coolant air precooling and fuel preheating on gas turbine cycle efficiency, power production, coolant mass flow and turbine exhaust temperature (TET) is evaluated. These help to compare different methods to increase power and efficiency of gas turbine cycle and also to predict the ultimate performance of current technology gas turbines.

In order to evaluate steam cycle performance, an upper and lower bound for TET is considered and all of possible HRSG layouts and pressure levels are considered to compare influence of gas turbine selection criteria on heat recovery and power production in steam cycle. Different formulations for modeling of HRSG are used based on superheater temperature of low pressure sections and high pressure saturation temperatures.

MODELING OF GAS TURBINE CYCLE

Simple cycle gas turbine as shown in fig (1) is considered for the present analysis. The cycle consists of a compressor, a combustion chamber and a cooled turbine. Modeling of gas turbine cycle is presented below.

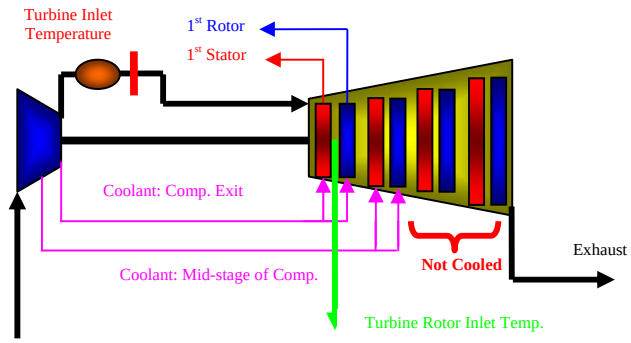

Fig (1) - Schematic Diagram of a Cooled Gas Turbine

- COMPRESSOR

Inlet air is composed of mole fractions of five ideal gas mixtures of N2, O_2, H_2O, CO_2 and Ar at ISO condition. For one kilogram of inlet air to compressor, entropy change can be written as [12]:

$$ds = \bar{c}_{PM}\frac{dT}{T} - R\frac{dP}{P} \quad (1)$$

Using the concept of polytropic efficiency, final exit temperature can be determined as:

$$\bar{c}_{PM}\frac{dT}{T} = \frac{R}{\eta_{\infty c}}\frac{dP}{P} \quad (2)$$

By integrating this equation (with C_{PM} function of temperature and mixture composition), exit condition can be determined numerically. But compressor work consumption can not be determined till blade cooling air and its location is determined. As will be described later, two options for coolant air extraction will be considered. Compressor work consumption is computed using the following formulation [12]:

$$W_c = m_{ex\_comp}.h_{ex\_comp} + \sum m_i.h_i \quad (3)$$

In the above formula, enthalpy is calculated relative to ambient temperature and subscripts i refers to coolant air extraction locations.

- COMBUSTION CHAMBER

Inlet fuel (natural gas) is composed of CH_4, C_2H_6, C_3H_8 and C_4H_{10}. Exit temperature of combustion chamber is an input to the model and then fuel consumption is calculated. Using thermodynamic laws, combustion equation can be written as:

$$\begin{aligned}&\bar{\lambda}(aC_{x1}H_{y1} + bC_{x2}H_{y2} + cC_{x3}H_{y3} + dC_{x4}H_{y4}) + \\ &(y_{O_2}.O_2 + y_{N_2}.N_2 + y_{Ar}.Ar + y_{CO_2}.CO_2 + y_{H_2O}.H_2O) \\ &\rightarrow (y_{CO_2} + \bar{\lambda}.n_{\alpha t}).CO_2 + (y_{H_2O} + .5n_{\beta t}.\bar{\lambda}).H_2O \\ &+ y_{N_2}.N_2 + y_{Ar}.Ar + (y_{O_2} - B.\bar{\lambda}).O_2\end{aligned} \quad (4)$$

Where $\bar{\lambda}$ is:

$$\bar{\lambda} = \frac{n_{fuel}}{n_{air}} \quad (5)$$

a, b, c and d are molar ratios of inlet fuel to combustion chamber, y_i is the molar ratio of inlet air, $n_{\alpha t}$ and $n_{\beta t}$ are sum of the carbon and hydrogen moles in the fuel. B is $n_{\alpha t} + 0.25 * n_{\beta t}$, and finally, $\bar{\lambda}$ can be written as [12]:

$$\begin{aligned}\bar{\lambda} = &\left[\begin{array}{l} y_{N_2}.\Delta\bar{h}_{N_2} + y_{O_2}.\Delta\bar{h}_{O_2} + y_{Ar}.\Delta\bar{h}_{Ar} \\ + y_{CO_2}.\Delta\bar{h}_{CO_2} + y_{H_2O}.\Delta\bar{h}_{H_2O}\end{array}\right]_{T_{exit\_compressor}}^{Tflame} \\ &/[LHV + \sum_{i=1}^{4} a_i.\Delta\bar{h}_{C_{xi}H_{yi}} \uparrow_{298.15}^{T_{fuel\_in}} - n_{\alpha t}.\Delta h_{CO_2} \uparrow_{298.15}^{T_{flame}} \\ &- .5n_{\beta t}.\Delta\bar{h}_{H_2O} \uparrow_{298.15}^{T_{flame}} + B.\Delta\bar{h}_{O_2} \uparrow_{298.15}^{T_{flame}}]\end{aligned} \quad (6)$$

LHV is the lower heating value of fuel. Then fuel air ratio based on mass flow can be written as:

$$f_{theoretical} = \frac{m_{fuel}}{m_{air}} = \frac{n_{fuel}}{n_{air}}.\frac{MW_{fuel}}{MW_{air}} = \bar{\lambda}.\frac{MW_{fuel}}{MW_{air}} \quad (7)$$

Actual fuel air ratio will be determined with combustion chamber efficiency as:

$$\eta_{C.C.} = \frac{f_{theoreticd}}{f_{actual}} \quad (8)$$

A correct value for state-of-art of gas turbines is between 0.99 and 0.997. Molar ratio of combustion products and mass flow entering turbine are determined at the exit of combustion chamber.

COOLED TURBINE MODEL

Cooled turbine model is based on El-Masri's works [13, 14] which has been modified and re-used by Bolland [15]. In this Model, blade temperature is an input (usually 1123K) and expansion path is considered to be continuous, instead of actual expansion (stage by stage expansion) [16]. The expansion path is divided into a large number of sub-stages, with the sequence of adiabatic expansion, total temperature and total pressure loss, both due to mixing of coolant and hot gases. This model has been applied where parametric analysis of gas turbine is our goal and the knowledge of expansion path is not important. However, such a model can not deliver information about expansion path.

For the element of the expansion path as shown in Fig. 2 and the expansion line in Fig. 3, the work extracted through the walls is given by:

$$d\dot{W} = -\dot{M}_g dH_g \quad (9)$$

For this element, the exit temperature of adiabatic expansion is found using polytropic efficiency of adiabatic turbine (similar to compressor exit temperature calculation) and the temperature after mixing with coolant air using energy equation; while care must be taken into account that work extraction process is an adiabatic process, if we use first law of thermodynamic for the whole element, reduced polytropic efficiency must be used instead of adiabatic efficiency due to mixing of coolant air and the main gas flow [12].

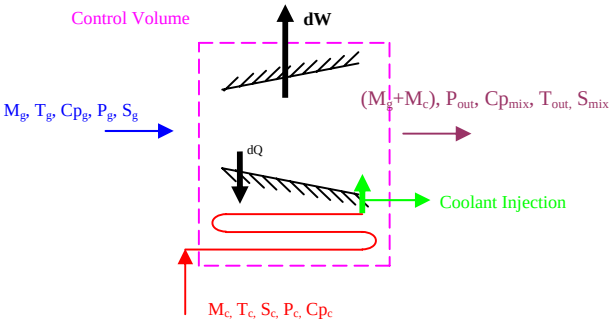

Fig (2) - Element of the cooled expansion path for continuous model

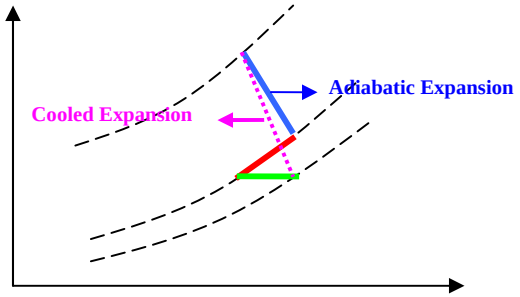

Fig (3) - Element of the cooled expansion path for continuous model

By combining the relations between work extraction and heat transfer for an element, the required coolant mass flow for each step is found from [12]:

$$\frac{d\dot{M}_c}{\dot{M}_g} = -\sigma\frac{dH_g}{T_0}\frac{(T_g - T_b)_g}{(H_b - H_c)_c} \quad (10)$$

Where σ is the parameter that characterizes the relative heat to work loadings on the machines surfaces and found by:

$$\sigma = \frac{St(A_{w,stage}/A_g)}{C.(k-1).M_a^2.\varepsilon} \quad (11)$$

The cooling efficiency ε is:

$$\eta_c = \frac{T_{c,e} - T_{c.i}}{T_b - T_{c,i}} \quad (12)$$

Total pressure loss due to coolant injection in hot gas flow is taken into account by means of the following equation:

$$\frac{dP}{p} = -\frac{d\dot{M}_c}{\dot{M}_g}k.M_a^2 Y \quad (13)$$

In this model, as mentioned, blade temperature is an input to the model (usually 1123 for F and G class of gas turbines). High values of σ (i.e. 0.4) refer to low blade cooling technology and reversely for high values of σ. A discussion on

best values for σ and T_b will be done in validation part of the paper.

MODELING OF DIFFERENT LAYOUTS OF HRSG

In this paper, Different layouts for HRSG will be modeled. In order to model HRSG, ***IAPWS*** (International Association for Properties of Water and Steam) standard for properties of water and steam has been used [17]. Two and three pressure HRSG with and without reheat is modeled.

Figure (4) shows the T-S diagram for a two pressure HRSG. For a known gas turbine exhaust condition (Temperature, mass and composition) and a set of HP and LP section inputs, LP and total mass flow and stack temperature will be determined by writing energy equation between gas turbine exhaust and HP, LP and stack. When writing these equations, based on the value of LP superheater outlet temperature and HP saturation temperature, two different expressions must be used. If $T_{sup,\ LP} > T_{sat,\ HP}$, (the case of mild reheat) then:

A=fraction of energy used to heat steam at or above $T_{sat,\ HP}$

$$= \frac{m_H.(h_{\sup,HP} - h_{wec,HP}) + m_L.(h_{\sup,LP} - h_{\sup,LP,TsatHP})}{q_{st}} \quad (14)$$

Where

$$q_{st} = m_L.(h_{\sup,LP} - h_{wec,LP}) + (h_{wec,LP} - h_{inec,LP}) + m_H.(h_{\sup,HP} - h_{inec,HP)}) + blowdown \quad (15)$$

$$blowdown = BD_{LP}.(h_{f,LP} - h_{inec,LP}) + m_H.BD_H.(h_{f,HP} - h_{inec,HP}) \quad (16)$$

B=fraction of energy used to heat steam at or above $T_{sat,LP}$

$$= \frac{q_{st} - [(h_{wec,LP} - h_{inec,LP}) + BD_L.(h_{f,LP} - h_{inec,LP})}{q_{st}} \quad (17)$$

The ratio of A to B is equal to:

$$\frac{A}{B} = \frac{h_{ex,GT} - h_{g,PPHP}}{h_{ex,GT} - h_{g,PPLP}} \quad (18)$$

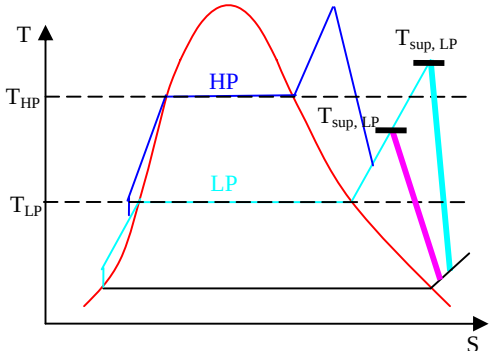

Fig (4) – T-S diagram for two-pressure steam cycle for two possible $T_{sup,\ LP}$

By dividing equations 14 and 17 and equaling them to 18, LP and HP mass flow will be determined. Then using one of 14 or 17, stack temperature will be determined. If $T_{sup,LP} < T_{sat,HP}$, then the only difference in calculations is in equation 14 where the right hand side of the nominator will be cut [12].

In all above equations, it was assumed that total mass flow enters LP economizer and HP pump is used after the LP economizer. The schematic diagram of HRSG is shown in fig (5). It must be emphasized that heat and mass balance is independent of HRSG layout between HP and LP evaporators and also after HP.

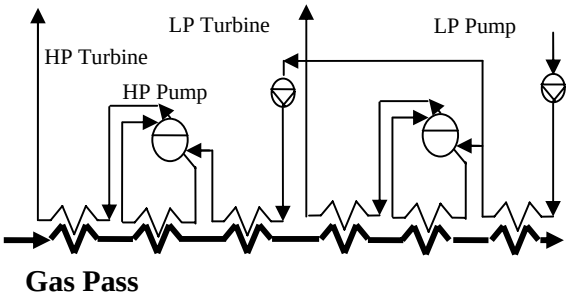

Fig (5) – one possible layout for two pressure HRSG

For two pressures with reheat cycle, the number of different situations is 4. Figure (6) shows reason of this. Due to mixing of HP turbine exit flow with LP superheater exit, a mixing occurs. Based on values of $T_{sat,\ HP}$, $T_{sup,\ LP}$ and T_{mix}, four different conditions occur (for $T_{sup,\ RH} > T_{sat,\ HP}$). They are as bellows:

(1) $T_{MIX} < T_{sat,\ HP}$ and $T_{sup,\ LP} < T_{sat,\ HP}$ (fig (6))
(2) $T_{MIX} < T_{sat,\ HP}$ and $T_{sup,\ LP} > T_{sat,\ HP}$
(3) $T_{MIX} > T_{sat,\ HP}$ and $T_{sup,\ LP} < T_{sat,\ HP}$
(4) $T_{MIX} > T_{sat,\ HP}$ and $T_{sup,\ LP} > T_{sat,\ HP}$

According to the procedure described for two pressure cycle, these four cases will be solved to determine all of the possible conditions for two pressure reheat cycle. When solving these equations together, in the first iteration, value of T_{MIX} will be guessed and then it will be checked to correct first guess [12].

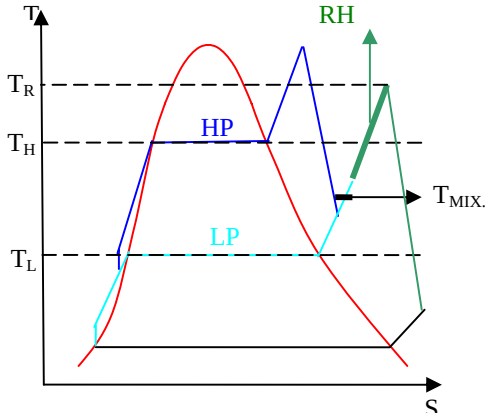

Fig (6) – T-S diagram for two-pressure reheat steam cycle of case (1)

For three pressure cycle, there 4 situations for energy balance between gas turbine exhaust and HP pinch point and 2 option for gas turbine exhaust and IP pinch point. Considering feasible conditions, 6 different conditions occur. For the purpose of simplicity, these conditions not are introduced here. For three pressure with reheat cycle, 10 possible situations occurred [12].

Because in the concept of heat recovery in a heat exchanger, first law efficiency is 100% (based on the ratio of heat rejection of hot stream to heat absorption of cold stream), therefore second law efficiency is used to determine HRSG efficiency. HRSG efficiency based on the ratio of total heat absorbed by water and steam to the all possible heat abruption (cooling the

gas to ambient temperature) is not a useful concept, because this does not compare quality of heat recovery in HRSG.

To determine second law efficiency of HRSG, two approach can be consider, first based on the whole amount of exergy decrease in gas side to amount of exergy increase in water side, and second by detail exergy analysis of all heat exchangers in HRSG. The second method of course yields more comprehensive results, but in order to consider that, the detail arrangement of the HRSG must be determined. When mass flow and stack temperature determined in all pressure levels, different arrangement can be selected between two pressure levels. It can be seen in fig. (7) that how two HP economizer and two LP superheater can be used in HRSG instead of one economizer and one superheater. Selection of the optimum configuration can be done using thermoeconomic and combined pinch and exergy approach [12]. This is not our interest in this paper, so the general exergetic analysis will be done here. This is defined as:

$\eta_{II,HRSG}$=exergy increase in cold side/exergy decrease in hot side (19)

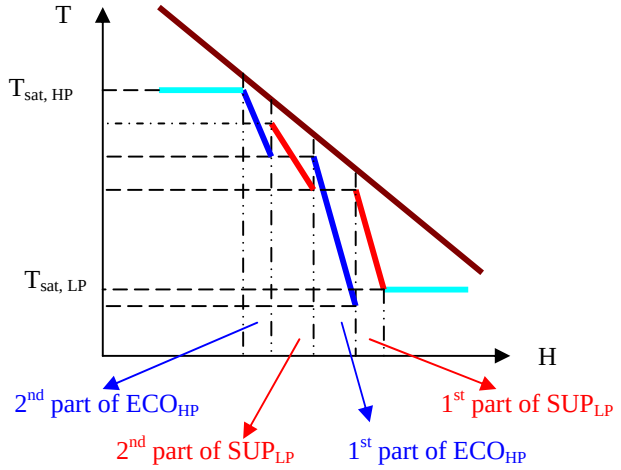

Fig (7) – one possible arrangement for LP superheaters and HP economizers

MODEL VALIDATIONS

Based on the later models, a computer code has been developed to analyze gas turbine and combined cycles. In order to validate gas turbine model, a large number of gas turbine cycles in different range of power, TIT and CPR is selected (table (1)). The inputs for DP are: DP_{inlet}=0.01, $DP_{c.c.}$ =0.04, DP_{exh}=0.02 for all turbines. Table (2) shows compressor, turbine and coolant mass flow per compressor inlet flow. Table (3) shows calculated and actual data for power, efficiency and TET for these turbines. Inputs for combustion chamber, mechanical, generator and gear box efficiencies are chosen from table (4). Values of σ, T_b and turbomachinary efficiencies is selected in a manner to minimize errors of efficiency, power and TET. It can be seen that for large heavy duty gas turbines, high blade cooling technology (low σ, i.e. between 0.1-0.2) and high values of T_b and turbomachinary efficiencies must be used.

The results show good agreement with manufactures data and it can be used for comparative evaluation of gas turbine cycle. This model is also validated for some other turbines in [18].

Table (1) –different gas turbines with model inputs

Gas turbine model	$\eta_{p,c}$	$\eta_{p,t}$	T_b	σ	CPR	TIT (K)	M_{in_c} (kg/s)
GE 5371 PA	0.894	0.875	1010	0.4	10	1237	122.1
GE 9171 E	0.9	0.885	1090	0.25	12.34	1397	405
GE 9351 FA	0.92	0.9	1123	0.18	15.85	1600	629.25
Siemens W 501 G[a]	0.908	0.9	1123	0.15	19.25	1698	544.9
Siemens W251 B10A[b]	0.895	0.88	1050	0.25	14.24	1367	156.3
Siemens V94.2	0.918	0.905	1080	0.3	11.44	1422	494.8
Hitachi H25[c]	0.92	0.9	1060	0.28	14.65	1545	86.9
Siemens V94.3A	0.908	0.9	1123	0.15	17.06	1589	635.8

a: CAP=200°C
b: coolant from compressor end, CAP=150°C
c: Coolant from compressor end

Table (2) – model outputs for compressor, turbine and CMF

	W_{comp} (MW)	W_{tur} (MW)	M_c/M_{in} (%)
GE 5371 PA	38.3	65.3	6.6
GE 9171 E	141.9	267.7	6.3
GE 9351 FA	242	502.8	11.3
Siemens W 501 G	235.2	482.8	12.17
Siemens W251 B10A	60.5	103.5	7.4
Siemens V94.2	160	319	10.1
Hitachi H25	32.84	60.56	19.06
Siemens V94.3A	260.8	527.6	8.75

Table (3) – model outputs for power, efficiency and TET

	W_{net} (MW)		Efficiency (%)		TET (K)	
	Cal.	Act.	Cal.	Act.	Cal.	Act.
GE 5371 PA	26.9	26.13	28.85	28.7	749	761
GE 9171 E	125.7	123.76	34.1	33.98	814	817
GE 9351 FA	260.7	256	37.9	37.5	870	879
Siemens W 501 G	247.7	248.4	39.3	39.2	882	869
Siemens W251 B10A	41.1	41.7	32.5	32.05	767	780
Siemens V94.2	159	156.5	34.39	34.39	821	823
Hitachi H25	26.36	26.63	32.8	32.92	832	831
Siemens V94.3A	266.7	262	38.78	38.62	858	861

Table (4) – inputs for mechanical and generator efficiency

Power (MW)	$\eta_{C.C.}$	$\eta_{mech.}$	$\eta_{gen.}$	$\eta_{g.b.}$
<1.5	0.99	0.98	0.95	0.98
1.5-5	0.99	0.98	0.96	0.98
5-10	0.992	0.985	0.97	0.985
10-25	0.993	0.988	0.97	0.985
25-50	0.994	0.99	0.98	0.985
50-100	0.996	0.992	0.985	0.985
>100	0.997	0.994	0.988	0.985

Validation of HRSG model is described in [19] and will not be expressed again.

RESULTS AND DISCUSSION

Results are expanded in two parts, the first one for gas turbine and second for steam cycle. In gas turbine results, we focus on effect of TIT, CPR, turbine blade cooling technology, coolant extraction location, Coolant Air Precooling (CAP) and fuel Preheating (FPH) on performance of gas turbine cycle. In steam cycle section, we consider two bound for gas turbine exhaust condition. The upper bound is for one large gas turbine with high exhaust temperature (future gas turbines) and the lower for medium size gas turbine.

-GAS TURBINE

Gas turbine in ISO condition is considered here with the following inputs. Fuel=CH_4, η_{pc}=0.905, η_{pt}=0.9, $\eta_{c.c}$=0.995, DP_{inlet}=0.01, DPc.c. =0.04, DP_{exh}=0.03. Effect of important parameters on design of gas turbine will be described here.

Fig (8) shows variation of efficiency and power with variation of TIT (1300-1700), CPR (5-25) and blade cooling technology (0.1-0.3). Here the whole coolant will be extract from compressor end (CEE: Compressor End Extraction). As can be seen, in high blade cooling technology (σ=0.1), increasing TIT first cause to increase in efficiency and power (1300-1500), while for the rest, it decreases efficiency. In weak blade cooling technology (σ=0.3), increasing TIT always decreases efficiency (different from σ=0.1), also increase in power is less than high blade cooling technology. Another interesting feature is that both power and efficiency for the case of TIT=1700K and σ=0.3 are less than the case of TIT=1500K and σ=0.1. This shows that when CEE is used, high blade cooling technology has more effect on power and efficiency than increasing TIT. For example, In Hitachi H25, using higher blade cooling technology instead of increasing TIT to 1545 K will be more useful. It is due to the high amount of the coolant that will be extracted from the compressor end at high temperature and pressure.

Fig (9) shows the variation in Coolant Mass Flow (CMF) with variation in CPR for CEE and CME cases in σ=0.1. As it is expected, in all of the cases, coolant mass flow for CEE case is higher relative to CME due to higher coolant temperature in CEE. This difference is higher in high TIT. With increasing CPR, compressor air exhaust temperature increase and more coolant is need to cool the turbine blades, therefore mass flow difference between CEE and CME increase with increase in CPR. The trend is similar for σ=0.3.

Fig (10) shows that for low blade cooling technology (σ=0.3), CME improves gas turbine power output significantly relative to CEE due to lower coolant extraction. This indicates that power output for the case of TIT=1700K and CEE is equal (except for high CPR) to the case of TIT=1500K and CME, while blade cooling technology is kept constant (σ=0.3). Therefore it can be concluded that in high values of σ, power increase due to coolant extraction point modification is equal to increase in TIT (200K). But for low σ (e.g. 0.1), CME has lower effect on power and TIT increment has higher effects.

In order to analyze variation of efficiency and power of CME case with major cycle parameters, consider fig (11). It shows different trend for both power and efficiency in high TIT respect to fig (8), but for the case of TIT=1300K, there is no major difference between CME and CEE cases. Maximum power for TIT=1700K and σ=0.1 increase more than 13% relative to CEE (fig (8)). Also because of lower coolant mass flow (fig. (9)), optimum CPR for maximum power increases relative to CEE. For low values of σ, increasing TIT increase both power and efficiency (different with CEE case). For higher values of σ, increasing TIT, increase efficiency in high CPR and decrease it at lower CPR (1300-1500) but for the rest, efficiency reduces. Also power output in TIT=1700K and σ=0.3 has similar values to TIT=1500K and σ=0.1(due to high coolant mass flow difference between these two cases (fig (12)), but the efficiency for the first case is lower (in the first case, combustion chamber air mass flow is lower than second case, but due to higher TIT, fuel mass flow will be higher and efficiency decrease).

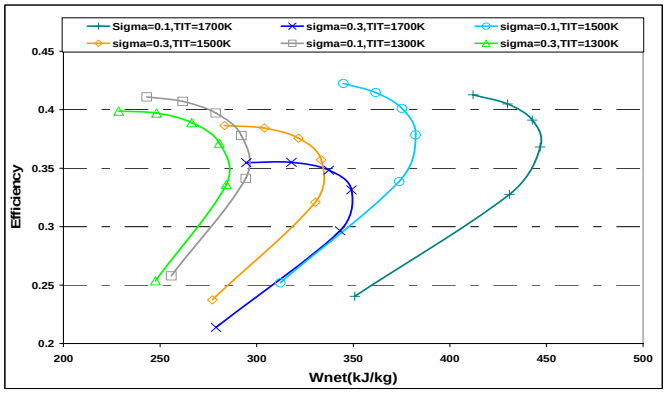

Fig (8) – variation of power and efficiency with TIT, CPR and σ for CEE

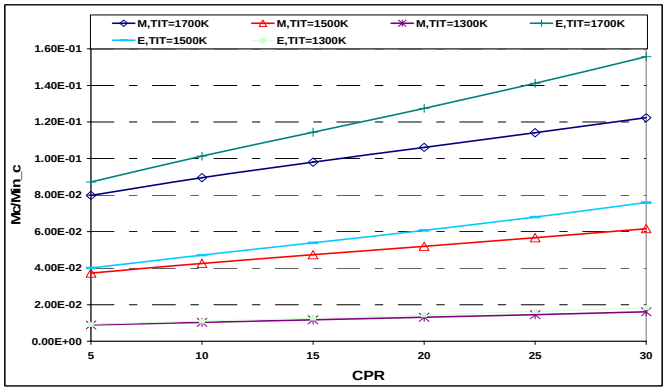

Fig (9) – variation of CMF with TIT and CPR for CEE and CME

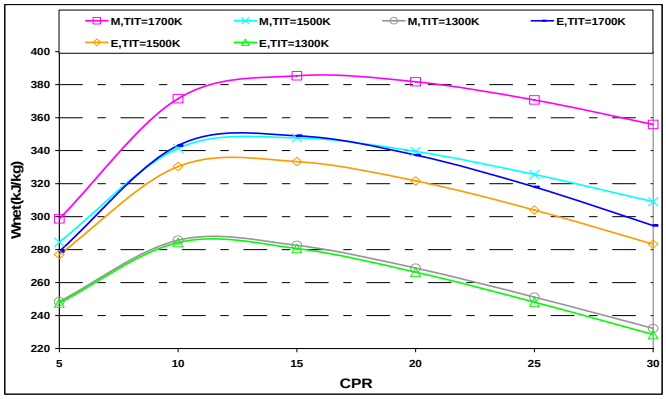

Fig (10) – variation of power output with CPR in different TIT for CEE and CME in σ=0.3

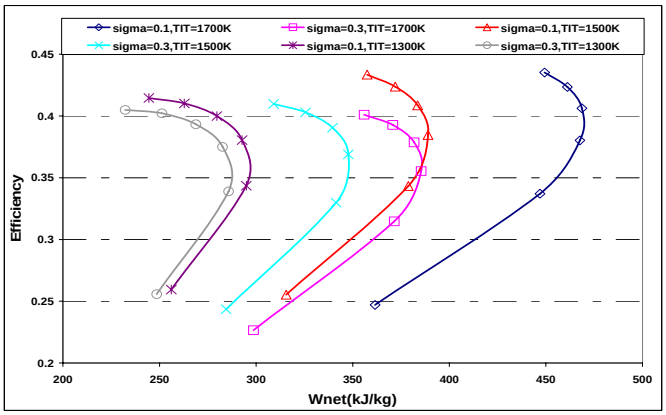

Fig (11) – variation of power and efficiency with TIT, CPR and σ for CME

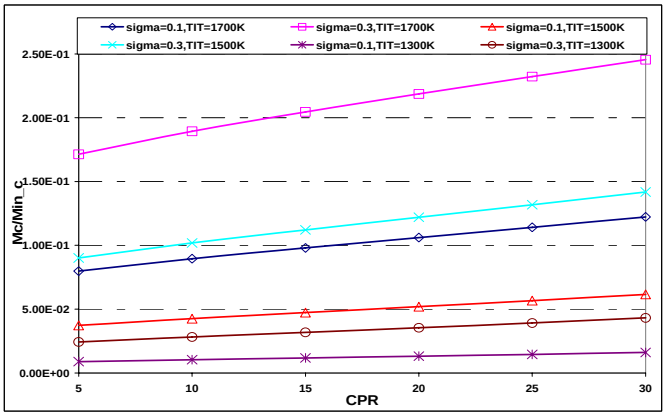

Fig (12) – variation of CMF with TIT and CPR for CME in σ=0.1. 0.3

Improving blade cooling technology also increase gas turbine exhaust temperature that has great effect on steam cycle power output. As can be seen in fig (13), for TIT=1700K and in all CPR's, exhaust temperature for σ=0.1 is higher about 40K relative to σ=0.1. But this difference is lower for lower TITs.

As described, CME reduces coolant temperature that is need to cool turbine mid stages. It decrease compressor work and increase turbine power. But first stage of turbine consumes a large faction of cooling mass flow and there is no difference between CME and CEE methods for the first stage. Precooling of the first stage coolant reduces coolant mass flow according to equations 10-12. Actually for a fixed designed gas turbine (without any change in coolant type, T_g and T_b), the only method to decrease coolant mass flow is decrease in coolant temperature. Coolant air precooling a little decrease C_{pc} (increase in M_c), but on the other hand reduce coolant enthalpy and the net effect is decrease in coolant mass flow. Fig (14) shows that precooling of coolant air reduces CMF significantly. With CEE case and CAP=200, CMF is lower than CME and CAP=0. Therefore, without using the problems for different location for coolant extraction and only with precooling, CMF will be lower than CME case. The only effect that does not allow power and efficiency of CEE case reach CME, is CEE high temperature for turbine mid stages relative to CME. It seems that with CAP for mid stages, power and efficiency can reach CME. Another important note is that with increasing CAP, the rate of CMF reduction decreases for CEE while increases for CME.

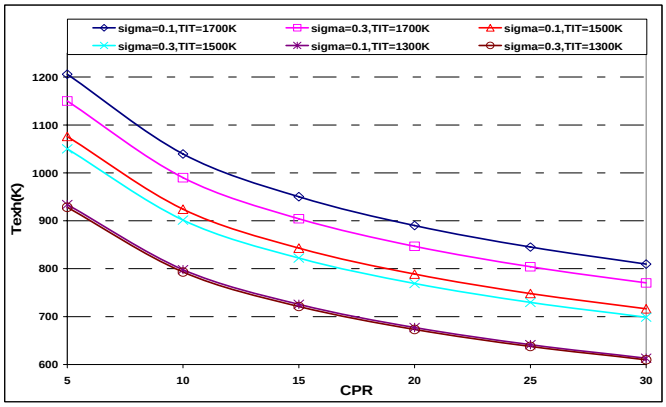

Fig (13) – variation of T_{exh} with CPR for Different TIT and σ

Figures (15) and (16) show effect of CAP on power and efficiency of gas turbine cycle. As can be seen, for medium TIT (1500 K), due to less CMF, CAP increases power less than high TIT and for CME; always CAP has less positive effect relative to CEE.

CAP reduces CMF and increase combustion chamber inlet air. Therefore in a specified TIT, it increase fuel flow rate and the gain in efficiency is lower than power. Actually CAP cause to small reduction in efficiency, but this negative effect can be compensated by fuel preheating with heat rejection of CAP. This increases efficiency of gas turbine cycle with reduction in fuel mass flow. Fig (17) shows effect of CAP and FPH on gas turbine cycle efficiency compared with the simple cycle efficiency. In all cases this causes to increase efficiency while power output also has been increased.

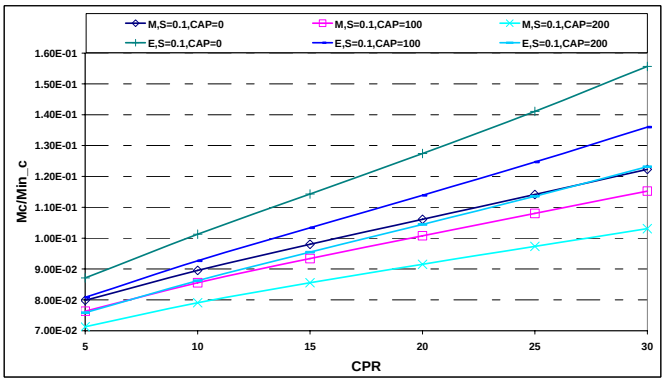

Fig (14) – variation of CMF with CPR for different TIT, CAP and coolant location extraction

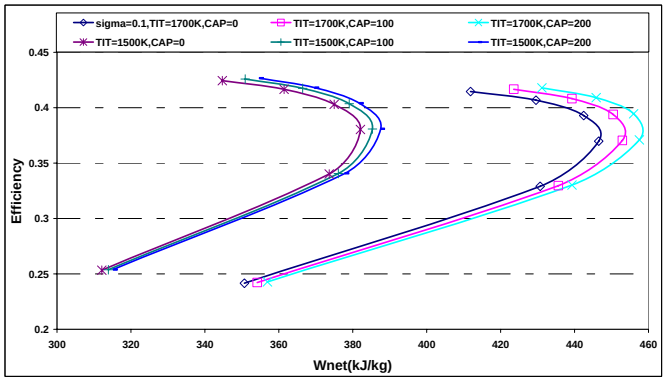

Fig (15) – variation of power and efficiency for CEE and CAP

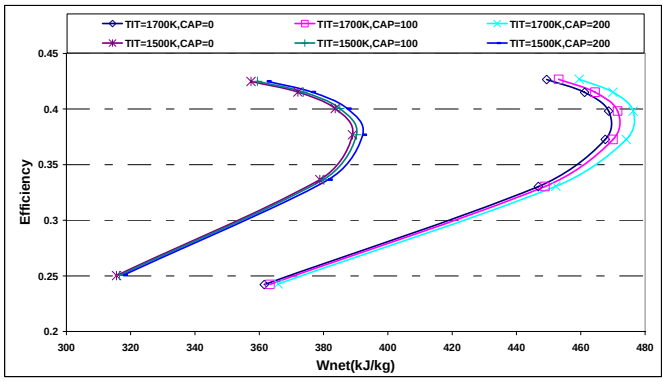

Fig (16) – variation of power and efficiency for CME and different CAP

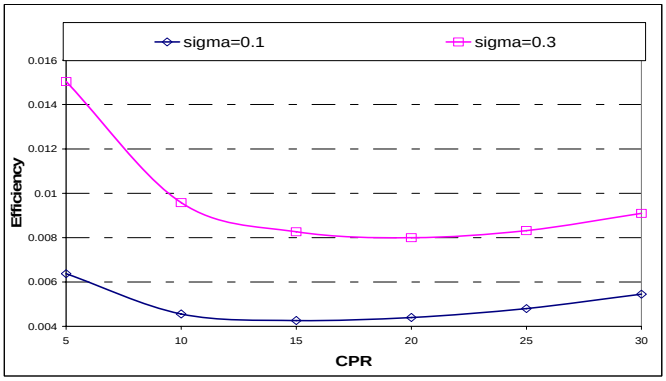

Fig (17) – variation of efficiency for CAP and FPH

-STEAM CYCLE

In order to evaluate and compare different layouts for steam cycle, instead of using exhaust temperature of a specified gas turbine cycle, two bounds for gas turbine exhaust temperature are considered. In the latest studies for evaluation of combined cycles, more attention is made to enhance gas turbine cycle efficiency [6] and [7], while no attention is made to evaluate or optimize different steam cycles for the gas turbines, or it only is done for a specified gas turbine exhaust condition [8], [20]. The important parameter in evaluation of steam cycles is power output, because for a specified gas turbine exhaust condition, increasing power output increase combined cycle efficiency directly.

As mentioned, the upper bound is kept constant with TET=950K and M_{exh}=700kg/s. This can be evaluated as the highest exhaust condition for the near future gas turbines. Based on the knowledge of the authors, maximum TET is for GT24/26 of ALSTOM/ABB power with 910K. Therefore, selection of this temperature can be a reasonable selection for near future gas turbines. The lower bound selected to TET=750K, and M_{exh}=500 kg/s. this is the conditions of a medium size E or F class exhaust temperature gas turbine. Other inputs for steam cycle are listed in table (4). Maximum dryness factor for steam turbine output is kept 0.88 and pressure increase will be stopped reaching this value. Figures for T_{exhgt}=950 K are on the left and for T_{exhgt}=750 K on the right hand side of the plots.

Fig (18) shows effect of variation power output of steam cycle with variation in steam cycle pressure for 1P and 2P pressure level. For T_{exhgt}=950 K, increasing pressure level cause to increase in power output (maximum 4.3 %) and with increase in P_{LP} power output increases. For T_{exhgt}=750 K, minimum P_{LP} has the best effect on power. In this case, power output increase about 10 % respect to maximum 1P pressure and 11.3 % respect to maximum 2P pressure.

The reason for this different power variation for two exhaust condition is due to different gas turbine exhaust temperature. Steam turbine power output can be written as: $W_{ST}=E_{in\text{-}HRSG} - E_{out\text{-}HRSG} - \sum I_{HX} - \sum I_{T\&P}$ [12] where E refers to total exergy and I to irreversibility (HX: Heat Exchanger; T: Turbine and P: Pump). Increase in pressure level cause to reduction of exergy losses between gas and water ($\sum I_{HX}$) and if E_{out_HRSG} and $\sum I_{T\&P}$ do not change significantly, power output will increase. For high temperature gas turbine exhaust, increase in pressure level, does not change difference between hot and cold stream significantly, because the slope of the hot curve in T-H diagram is high (fig (19)) and in order to decrease differences and irreversibility and increase power, numbers of pressure levels must increase to high value, While for low temperature gas turbine exhaust, this difference reduce significantly with increase pressure levels (fig (19)).

Table (5) - inputs for steam cycle

$P_{cond.}$ (MPa)	0.007	$\eta_{is,\ PHP}$	0.8
ΔT_{PPHP}	20	$\eta_{is,\ PIP}$	0.8
ΔT_{PPIP}	20	$\eta_{is,\ PLP}$	0.8
ΔT_{PPLP}	20	$T_{sup,\ HP}$	840 (40 K less than T_{exhgt})
ΔT_{APHP}	5	$T_{sup,\ RH}$	840 (40 K less than T_{exhgt})
ΔT_{APIP}	5	DP_{eco}	0.03
ΔT_{APLP}	5	DP_{sup}	0.03
η_{isTHP}	0.889	DP_{RH}	0.07
η_{isTIP}	0.88	DP_{Pre}	0.03
η_{isTLP}	0.86	BD	0.01

In high T_{exhgt}, 2PRH cycles, always improve power output and on the contrary with 2P cycle, lower P_{LP} results in more power output. It occurs because lower LP pressure cause to more heat recovery in medium temperature region of the HRSG and more hot energy (more exergy) is available for the high pressure section. But for low T_{exhgt}, high values for P_{LP} reduces power output respect to 2P cycle. It means that in hot section of the HRSG, more heat is delivered to LP pressure heat exchangers. Again, similar to the 2P cycle, reheat with low pressure P_{LP} has more positive effect for low T_{exhgt} respect to high T_{exhgt}. Another important issue is that for high T_{exhgt}, there is no optimum for HP pressure from power production viewpoint or steam turbine exhaust wetness, but for low T_{exhgt}, an optimum occurs between 5.5-6.5 MPa and increasing the pressure more does not increase power output.

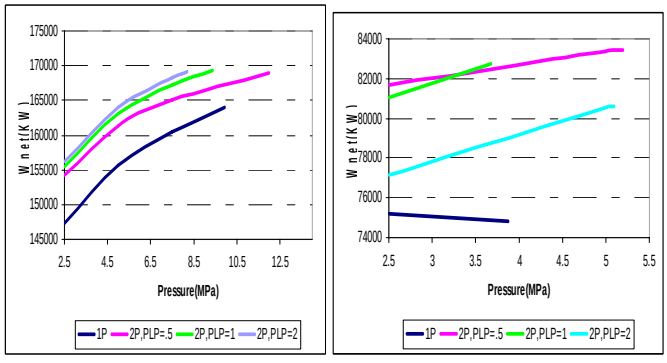

Fig (18) – variation of SC power output with P_{HP} for 1P and 2P cycle

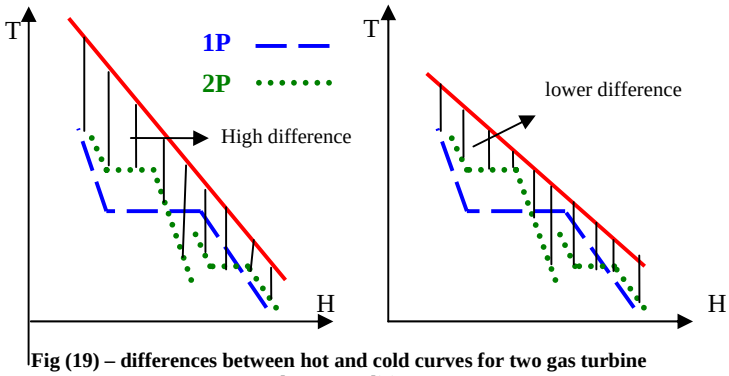

Fig (19) – differences between hot and cold curves for two gas turbine exhaust condition

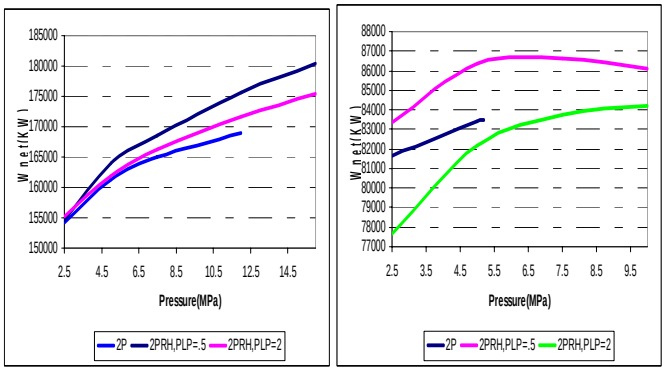

Fig (20) – variation of SC power output with P_{HP} for 2P and 2PRH cycle

Similar trends for increase pressure level from 2 to 3 occurs; more power increase for lower T_{exhgt}, more power for lower P_{LP} and no optimum HP pressure. As it can be seen, change from 2 to 3 pressure level, decrease P_{HP} due to wetness appearance in turbine exhaust, so mild reheat (increasing $T_{sup,IP}$ to $T_{sup,HP}$) can increase turbine dryness. But as can be seen in figure (22), increase in $T_{sup,IP}$ reduces power output in similar HP pressures due to increase in share of high exergy region of the HRSG for IP steam heating and reduce in HP steam mass flow. However, because of higher pressures that will be used in 3PM cycle, the final power output (in higher P_{HP}) will be higher than 3P cycle. It must be emphasized that negative effects of mild reheat for power is less for low T_{exhgt} because in this temperatures, exergy of hot gas is less than high T_{exhgt}, and the net effect will be less for it.

Figure (23) shows that in low P_{LP} and high P_{HP}, 3PRH power output increase significantly respect to 3P cycle (again more effect in low T_{exhgt}). Also for high T_{exhgt}, there is no optimum for P_{HP} but similar to 2PRH cycle, for low T_{exhgt}, an optimum pressure around 7.5 MPa maximize power.

In order to evaluate first and second law efficiency of HRSG, stack temperature must be determined. Fig (24) shows the stack temperature variations with HP pressure for different configurations in T_{exhgt}=950K. As can be expected, the higher stack temperature is for 1P cycle. Reducing P_{LP} in 2P cycle decrease T_{st} and increase first law efficiency of the HRSG (but decrease power output). 2PRH cycle has the highest stack temperature between multi pressure steam cycles. Also 3PPre (three pressure with preheating loop) cycle has the lowest stack temperature due to low pressure preheating loop. In the right hand side of fig (24) can be seen that there is no major difference between stack temperature of 2P, 3P and 3PRH cycle and also it can be concluded that the first law efficiency of HRSG will not change significantly between these cases. But there is large difference between power production of these cycles. It can be concluded that first law efficiency of HRSG can not help to detail evaluation of different pressure levels selection and their influence on quality of heat recovery and value of power production.

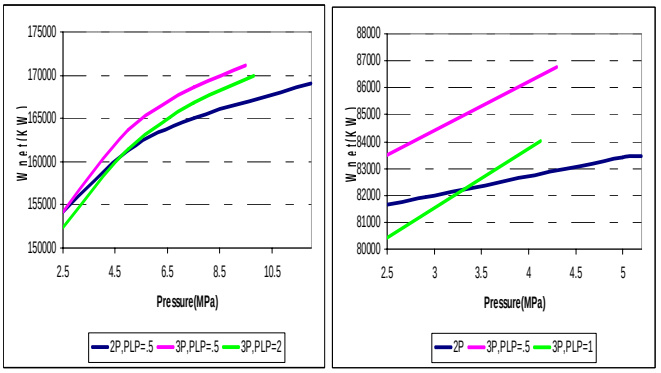

Fig (21) – variation of SC power output with P_{HP} for 2P and 3P cycle

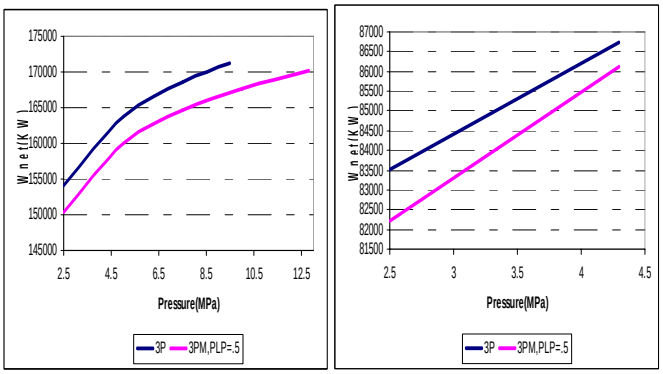

Fig (22) – variation of SC power output with P_{HP} for 3P and 3PM cycle

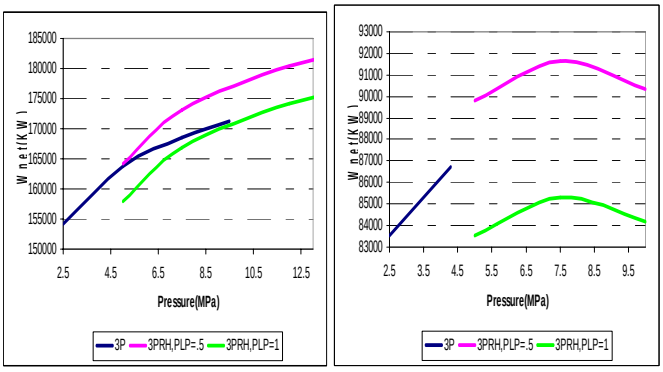

Fig (23) – variation of SC power output with P_{HP} for 3P and 3PRH cycle

Second law efficiency of HRSG can show a more actual view for it. Where second law efficiency growth, more exergy will be recovered (decrease in loss of heat exchanger network) and of course more power will be produced. Fig (25) shows that always cycles with low T_{exhgt} have higher second law efficiency (higher sensitivity to increase pressure level and higher increase in power production). As described, due to lower slope of the hot gas line in T-H diagram, increasing pressure level closes hot and cold curves more relative to higher T_{exhgt} where we need higher number of pressure levels to reduce exergetic losses. Also reheat cycles especially in high

pressure can reach about 90% second law efficiency which means good exergy recovery (more power produces in reheat cycles) while from first law viewpoint, it has similar efficiency with other multi pressure cycles. 2P, 3P and 3PM cycles have similar quantities for efficiency.

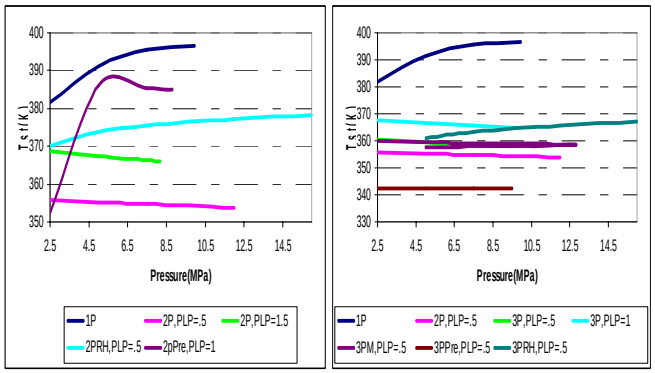

Fig (24) – variation of stack temperature with P_{HP} for different configurations

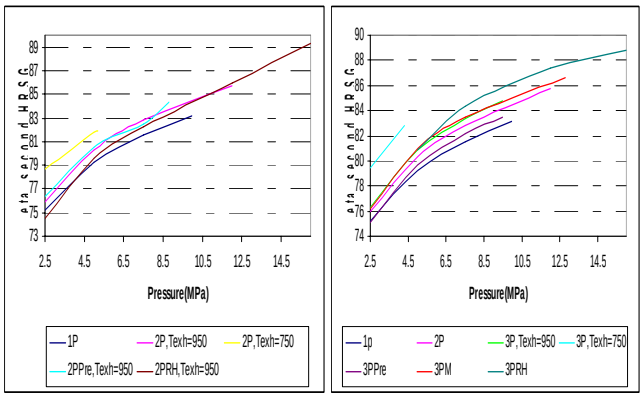

Fig (25) – variation of second law efficiency with different configurations and two gas turbine exhaust condition

CONCLUSIONS

In this paper, a thermodynamic model for evaluation of gas turbine and combined cycle was developed. Results of the model show good agreement with available data from manufacturers.

Using this model, change in major design parameters has been analyzed comprehensively for gas turbine and steam cycle separately. Main findings of this research are:

- For compressor exhaust extraction case, high blade cooling technology (low σ) has more effect on power and efficiency than increasing TIT due to the high amount of the coolant extraction from the compressor end at high temperature and pressure.
- In high values of σ, power increase due to coolant extraction point modification is equal to increase in TIT (200K). But for low σ, mid extraction has lower effect on power and TIT increment has higher effects.
- Increasing TIT higher than 1700K with current blade cooling technology (σ=0.1), there will be no other gain in efficiency (or decrease in its value) and only power increases.
- Coolant air precooling reduces coolant mass flow significantly. With coolant end extraction case and CAP=200, mass flow of coolant is lower than coolant mid extraction and CAP=0. For medium TIT (1500 K), due to less coolant mass flow, coolant air precooling increases power less than high TIT and for coolant mid extraction case; always CAP has less positive effect relative to end extraction.
- Coolant air precooling and fuel preheating in all cases increase efficiency while power output also has been increased.
- For high temperature gas turbine exhaust, increase in pressure level (2-3), does not change difference between hot and cold stream significantly, in order to decrease differences and irreversibility and increase power, numbers of pressure levels must increase to high value, While for low temperature gas turbine exhaust, this difference reduce significantly with increase pressure levels (2-3).
- For high gas turbine exhaust temperature, 2PRH and 3PRH configurations have no optimum HP pressure from power production viewpoint or steam turbine exhaust wetness, but for low gas turbine exhaust temperature, an optimum occurs between 5.5-6.5 MPa for 2P and 7.5 MPa for 3P configuration. They produce the maximum power between all cases.
- First law efficiency of HRSG will not change significantly for multi pressure configurations. Therefore, first law efficiency is not a good criterion for evaluation of different pressure levels and their influence on quality of heat recovery.
- Variation of second law efficiency is proportional with variation of power, where second law efficiency growth, more exergy will be recovered (decrease in loss of heat exchanger network) and more power will be produced.
- Reheat cycles in high pressure can reach about 90% second law efficiency which means good exergy recovery (more power occurs for reheat cycles) while from first law viewpoint, it has similar efficiency with other multi pressure cycles.

REFERENCES

[1]M.A. El-Masri, 1987, “Thermodynamic and Performance Projections for Intercooled/ Reheat/Recuperated Gas Turbine Systems”, ASME Gas Turbine conference, 87-GT-108

[2] K.Sarabchi, “Performance Evaluation of Reheat Gas Turbine Cycles”, Proc. Instn Mech. Engrs, Vol.218, Part A: J. Power and Energy

[3] B. Facchini, 1993, “New Prospects for use of Regeneration in Gas Turbine Cycles”, ASME Cogen Turbo Conference, IGTI-Vol.8.

[4] P .Chiesa, G .Lozza, E .Macchi, S .Consonni, 1995, “An assessment of the thermodynamic performance of mixed gas steam cycles: Part A-”, Journal of Engineering for Gas Turbines and Power, 117: 499–508.

[5] P .Chiesa, G .Lozza, E .Macchi, S .Consonni, 1995, “An assessment of the thermodynamic performance of mixed gas steam cycles: Part B—Water-injected and HAT cycles”, Journal of Engineering for Gas Turbines and Power, 117: 499–508.

[6] B.Facchini, D.Fiaschi, G.Manfrida, 2000, “Exergy Analysis of Combined Cycles Using Latest Generation Gas Turbines”, ASME J. of Eng. For Gas Turbine & Power, pp233
[7] Chiesa, P., and Macchi, E., 2004, ‘‘A Thermodynamic Analysis of Different Options to Break 60% Electric Efficiency in Combined Cycle Power Plants,’’ ASME J. Eng. Gas Turbine and Power, Vol.126, pp.770-785.
[8] C. Casarosa, A. Franco, 2001, “Thermodynamic Optimization of Operative Parameters for the heat recovery in combined Plants”, Journal of Applied Thermodynamics, 4(1):43-52.
[9] P. Chiesa, S. Consonni, G. Lozzo, E. Macchi, 1993, “Predicted the Ultimated Performance of Advanced Power Cycles Based on Very High Temperatures”, ASME Gas Turbine Conference, 93-GT-223.
[10] C. Casarosa, F. Donatini, A. Franco, 2004, “Thermoeconomic Optimization of Heat Recovery Steam Generators Operating Parameters for Combined Plants”, Journal of Energy, 29, 389-414
[11] A. Franco, C. Casarosa, 2004, “Thermoeconomic Evaluation of the Feasibility of Highly Efficient Combined Cycle Power Plants”, Journal of Energy, 29, 1963-1982.
[12] H.Khaldi, 2004, "Thermodynamic Modeling of Advanced Gas Turbine Combined Cycles with Application of Combined Pinch & Exergy Approach", M.S Thesis, Sharif Uni..
[13] M.A. El-Masri, 1986, “On Thermodynamics of Gas Turbine Cycles: Part 2” ASME J. of Eng. Gas Turbine & Power, pp.151-162.
[14] M.A. El-Masri, 1986 “On Thermodynamics of Gas Turbine Cycles: Part 3”, ASME J. Eng. Gas Turbine & Power, pp.162-173.
[15] O.Bolland, J.F.Stadaas, 1995, “Comparative Evaluation of Combined Cycles & Gas Turbine Systems with Water Injection, Steam Injection and Recuperation”, ASME J. Eng. Gas Turbine and Power, pp.138-147.
[16] M.A. El-Masri, 1986, "GASCAN: An Interactive Code for Thermal Analysis for Gas turbine Systems", ASME Winter Annual Meeting, C.A.
[17] F.Prini, 1997, “Release on International Association for Properties of Water and Steam (IAPWS) Industrial Formulation 1997 for Thermodynamic Properties of Water & Steam", Earlangen,
[18] H.Khaldi, R.Zomorodian, M.B.Ghofrani, K.Sarabchi, 2005, "Effect of Inlet Air Cooling by Absorption Chiller on Gas Turbine and Combined Cycle Performance", Proceeding of IMECE, November 5-11, Orlando, FL, USA
[19]M.A. El-Masri, 1987,"Exergy Analysis of Combined Cycles: Part 2", ASME J. Eng. Gas Turbine & Power, 109**,** pp.229-237.
[20] P.J. Dechampes, 1998, “Advanced Combined Cycle Alternatives with the Latest Gas Turbines”, ASME J. Eng. Gas Turbine and Power, pp.350-357